The EMBO Journal (2005) 24, 1911–1920 | © 2005 European Molecular Biology Organization | All Rights Reserved 0261-4189/05
www.embojournal.org

THE EMBO JOURNAL

The *macro* domain is an ADP-ribose binding module

Georgios I Karras[1,3,4], Georg Kustatscher[1,3], Heeran R Buhecha[1,2,5], Mark D Allen[2], Céline Pugieux[1], Fiona Sait[2], Mark Bycroft[2,*] and Andreas G Ladurner[1,*]

[1]Gene Expression Programme and Structural & Computational Biology Programme, European Molecular Biology Laboratory, Heidelberg, Germany and [2]MRC Centre for Protein Engineering and MRC Laboratory of Molecular Biology, Cambridge, UK

The ADP-ribosylation of proteins is an important post-translational modification that occurs in a variety of biological processes, including DNA repair, transcription, chromatin biology and long-term memory formation. Yet no protein modules are known that specifically recognize the ADP-ribose nucleotide. We provide biochemical and structural evidence that *macro* domains are high-affinity ADP-ribose binding modules. Our structural analysis reveals a conserved ligand binding pocket among the *macro* domain fold. Consistently, distinct human *macro* domains retain their ability to bind ADP-ribose. In addition, some *macro* domain proteins also recognize poly-ADP-ribose as a ligand. Our data suggest an important role for proteins containing *macro* domains in the biology of ADP-ribose.

The EMBO Journal (2005) **24,** 1911–1920. doi:10.1038/sj.emboj.7600664; Published online 19 May 2005
Subject Categories: structural biology; proteins
Keywords: ligand; metabolites; NAD; PARP; protein module

Introduction

There have been over 40 years of research into the biology of protein ADP-ribosylation (Chambon *et al*, 1963; Weill *et al*, 1963) and *in vivo* evidence suggests that this post-translational modification is important in gene expression. In particular, this occurs through the regulation of both chromatin structure and transcription in the nuclei of metazoan cells.

A variety of enzymes catalyze the addition of ADP-ribose onto proteins, either in the form of mono-ADP-ribosylation (mostly extracellular and cytoplasmic) or poly-ADP-ribosylation (Corda and Di Girolamo, 2003; Ame *et al*, 2004). Poly-ADP-ribose (PAR) polymerases are known as PARPs (D'Amours *et al*, 1999). Different classes of PARPs exist and their functions include DNA repair (Durkacz *et al*, 1980; Rouleau *et al*, 2004), transcriptional activation and repression (Kraus and Lis, 2003), telomere biology (Smith *et al*, 1998; Dynek and Smith, 2004), insulator activity (Yu *et al*, 2004), microtubule formation (Chang *et al*, 2004) and long-term memory (Cohen-Armon *et al*, 2004; Hanai *et al*, 2004).

Despite these critical functions, there is no molecular understanding of how these tightly associated and probably covalent (Ogata *et al*, 1980; Simonin *et al*, 1993; Kim *et al*, 1997; Ruf *et al*, 1998) post-translational modifications (PTMs) function. The best-characterized PARP is PARP1 (Benjamin and Gill, 1980; Ikejima *et al*, 1990; D'Amours *et al*, 1999). Its activity on histones (Poirier *et al*, 1982; Adamietz and Rudolph, 1984; Krupitza and Cerutti, 1989), transcription factors (Hassa and Hottiger, 1999; Cervellera and Sala, 2000) and other substrates is stimulated by single-strand DNA breaks. As a result of PARPs activity, the chromatin template may become more accessible.

Other PARPs maintain chromosome integrity at telomeres. These telomeric, ankyrin-repeat containing PARPs (tankyrases; (Smith *et al*, 1998; Cook *et al*, 2002; Rippmann *et al*, 2002) bind TRF1 and are required for mitotic progression to anaphase (Dynek and Smith, 2004). This suggests that poly-ADP-ribosylation is important for chromosome segregation. Various centromere proteins are, in fact, poly-ADP-ribosylated (Earle *et al*, 2000; Saxena *et al*, 2002).

PAR turnover is rapid and is catalyzed by PAR glycohydrolases (PARG) (Miwa and Sugimura, 1971), which can break PAR down to monomeric ADP-ribose (Lin *et al*, 1997; D'Amours *et al*, 1999; Winstall *et al*, 1999a, b; Davidovic *et al*, 2001). PARGs are thought to reverse the action of PARPs (Kraus and Lis, 2003) by lowering transcription and promoting chromatin condensation.

The dynamic nature of the PAR polymer rivals the enzymology of other reversible modifications, such as phosphorylation and acetylation. Similarly, poly-ADP-ribosylation plays a key role in epigenetics. PARP is required for the silencing of a *Drosophila* retrotransposon (Tulin and Spradling, 2003), for example, and in the imprinting of more than 140 CTCF target genes (Yu *et al*, 2004). In addition, PARP1 directly binds chromatin (Kim *et al*, 2004). Poly-ADP-ribosylation is therefore receiving increasing attention as an 'epigenetic' regulator (Kraus and Lis, 2003; Ladurner, 2003).

While roles for PAR have been identified, there is little information on the role of monomeric ADP-ribose. PARG-mediated breakdown of PAR leads to dramatically increased ADP-ribose concentrations. The drop in NAD^+ levels during PAR synthesis is followed by high concentrations of monomeric ADP-ribose shortly after. In both cases, specific signaling molecules could 'interpret' these metabolic states. Indeed, PARP and PARG function probably does have vital

*Corresponding authors. M Bycroft, MRC Centre for Protein Engineering and MRC Laboratory of Molecular Biology, Hills Road, Cambridge, CB2 2QH, UK. Tel.: +44 1223 402133; Fax: +44 1223 402140; E-mail: mb10031@cus.cam.ac.uk or AG Ladurner, Gene Expression Programme and Structural & Computational Biology Programme, European Molecular Biology Laboratory, Meyerhofstrasse 1, 69117 Heidelberg, Germany. Tel.: +49 6221 387 8156; Fax: +49 6221 387 8442; E-mail: ladurner@embl.de
[3]These two authors contributed equally to this work
[4]Present address: Max-Planck-Institut für Biochemie, Am Klopferspitz 18, 82152 Martinsried, Germany
[5]Present address: Trinity Hall, Cambridge CB2 1TJ, UK

Received: 29 October 2004; accepted: 6 April 2005; published online: 19 May 2005

connections to cellular NAD^+ homeostasis, as it has been suggested that DNA-damaged cells may undergo apoptosis as a result of the depletion in cellular NAD^+ (Chiarugi, 2002). As NAD homeostasis plays a role in ageing, there is an active interest in understanding the role of NAD metabolites. Several other cellular pathways produce ADP-ribose-like metabolites, such as the second messenger cyclic-ADP-ribose and ADP-ribose phosphate during tRNA splicing, but it is because of the connection between PAR, DNA repair and apoptosis, that PAR pathways have also been of pharmaceutical interest (Virag and Szabo, 2002; Beneke *et al*, 2004).

Yet no module capable of recognizing monomeric or polymeric ADP-ribose has been described. To search for candidate ADP-ribose and PAR binding modules, we have studied Af1521, a thermophilic protein containing a wide-spread and conserved $\pm$190-residue domain known as the *macro* domain (Aravind, 2001; Allen *et al*, 2003; Ladurner, 2003).

There are currently $\pm$300 proteins in the SMART database (Letunic *et al*, 2004) that contain a *macro* domain. Genomes with *macro* domains include pathogenic bacteria, such as *Salmonella typhimurium* (McClelland *et al*, 2001) and *Listeria* (Glaser *et al*, 2001), and ssRNA viruses, such as Rubella and Hepatitis E. In vertebrates, the domain can be found in genes with predicted PARP activity (Ame *et al*, 2004) (PARP9, PARP14 and PARP15), in a histone known as macroH2A (Pehrson and Fried, 1992; Chadwick and Willard, 2001; Allen *et al*, 2003; Ladurner, 2003), in a protein with predicted ATP-dependent chromatin remodeling activity and in a protein that may bind lipids through a Sec14-homology domain. Overall, the *macro* module may be used in diverse biological pathways. Here we show that Af1521 binds ADP-ribose with nanomolar affinity; further, we present two crystal structures for Af1521 bound to ADP-ribose and ADP, respectively. We extend our studies to human proteins and identify an interaction between *macro* domains and PAR. Our molecular data suggest a frontline biological function of *macro* domains in the recognition of monomeric and polymeric ADP-ribose.

Results

The Af1521 macro domain can hydrolyze a phosphoester

We have previously determined the structure of the *macro* protein Af1521 from the thermophilic organism *Archaeoglobus fulgidus* (Allen *et al*, 2003). A screen in the yeast *Saccharomyces cerevisiae* identified a protein with homology to the *macro* domain of Af1521, the YBR022W gene product, as exhibiting ADP-ribose-1″-phosphate (Appr-1″-P) processing activity (Martzen *et al*, 1999). Appr-1″-P is a metabolite produced by the action of a cyclic phosphodiesterase on a NAD^+ metabolite during tRNA splicing (Culver *et al*, 1993). The high-throughput screen did not identify the chemical identity of the product in the YBR022W-catalyzed reaction. We tested whether Af1521 may display activity on Appr-1″-P.

Using a TLC-based assay, we find that Af1521 hydrolyzes Appr-1″-P (Figure 1, lane 3). Further, the main product of the reaction has a mobility identical to that of ADP-ribose (Figure 1, lane 4), suggesting that ADP-ribose and inorganic phosphate are the two products of the reaction. Incubation of Appr-1″-P with calf intestine alkaline phosphatase generates a product with identical mobility to that of the Af1521-catalyzed reaction (data not shown).

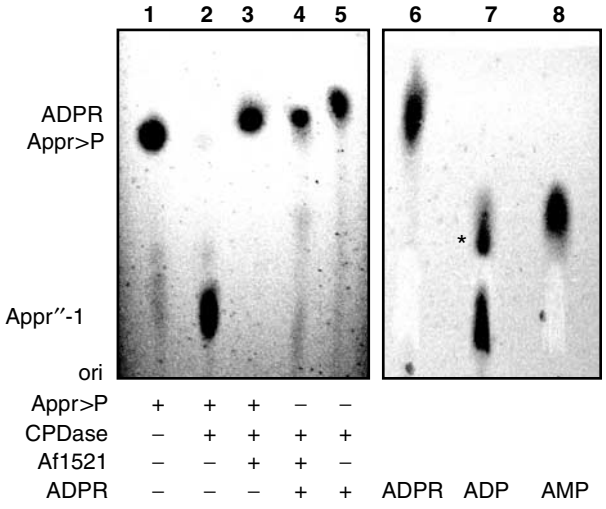

Figure 1 The Af1521 *macro* domain hydrolyzes a phosphorylated form of ADP-ribose. Thin-layer chromatography assays of Af1521-catalyzed reaction products. Lanes (1–5) contain reaction mixtures as indicated. Lanes (6–8) contain the indicated nucleotides in buffers identical to lane 3 but without Af1521 protein and without Appr > P. The asterisk denotes a breakdown product of ADP. Abbreviations are as follows: ADP-ribose (ADPR), ADP-ribose-cyclic-1″-2″-phospate (Appr > P), ADP-ribose-1″-phosphate (Appr-1″-P), origin of the chromatographic separation (ori) and cyclic phosphodiesterase (CPDase). Assays contained 2 mM Appr > P converted to Appr-1″-P using CPDase. To this mixture, we added Af1521 *macro* domain protein. Following incubation, the reactions were mixed with tetrabutylammonium and run on a Alugram Nano-SIL CN/UV_{254} TLC plate and using 1.5 M LiCl and 20% v/v ethanol in water. Fluorescence images were taken at 254 nm wavelength.

Consistent with hydrolysis of the 1″-phosphate of Appr-1″-P, the Af1521-catalyzed reaction produces inorganic phosphate (P_i). This is readily detected using a malachite green assay. Using 4.0 nmol of the precursor Appr > P (see Materials and methods), we obtain 2.9 nmol of inorganic phosphate (data not shown), suggesting hydrolysis of the Appr-1″-P to P_i and ADP-ribose. A GST-fusion of the YBR022W gene product also catalyzes the reaction, generating identical products (data not shown).

Our data indicate that the Af1521 and YBR022W *macro* domains hydrolyze Appr-1″-P to ADP-ribose and P_i.

The Af1521 protein binds ADP-ribose

The ability of Af1521 to catalyze phosphohydrolysis prompted us to test its ability to bind ADP-ribose. We measured the binding of ADP-ribose to Af1521 using isothermal titration calorimetry (Figure 2). The affinity of ADP-ribose for the Af1521 *macro* domain is high with a calculated equilibrium dissociation constant (K_D) of 126 ± 21 nM and a stoichiometry of 1:1 ($N = 0.91 \pm 0.01$; Table I). The ΔH for binding of ADP-ribose to Af1521 is -16.4 ± 0.2 kcal/mol, suggesting that ligand binding is coordinated by a number of noncovalent interactions.

We tested the selectivity of the Af1521 *macro* domain toward ADP-ribose using a range of related nucleotides. The K_D of the Af1521 *macro* domain for ADP is 5.6 ± 0.8 μM (Figure 3A; Table I; $\Delta H = -12.0 \pm 0.2$ kcal/mol). This suggests that the distal ribose of ADP-ribose makes important

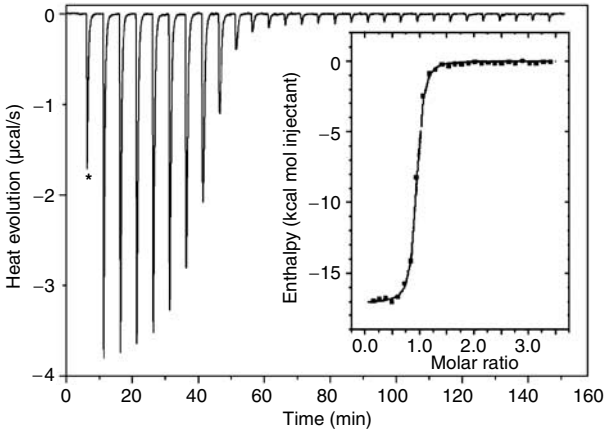

Figure 2 High-affinity binding of the *macro* domain to ADP-ribose. Isothermal titration calorimetry profile: Titration of ADP-ribose ligand into a solution containing the purified Af1521 *macro* domain. The asterisk denotes the first, small volume injection that is not used for subsequent data fitting. The inset shows the fit of the data to an equilibrium binding isotherm. The fit provides an equilibrium dissociation constant (K_D) for the binding of ADP-ribose to Af1521 of 126±21 nM.

Table I Binding of nucleotide analogs to the Af1521 *macro* domain

Ligand	K_D (μM)[a]	*N*	Δ*H* (kcal/mol)
ADP-ribose	0.13±0.02	0.93±0.01	−16.4±0.2
ADP	5.63±0.76	0.98±0.01	−12.0±0.2
AMP	38.0±4.0	0.90±0.10	−9.7±1.1
ATP	18.7±4.1	0.97±0.05	−6.1±0.6
Adenosine	>100	ND	ND
NAD	>100	ND	ND
GDP	>100	ND	ND

Equilibrium values for binding of nucleotide analogs were determined by isothermal titration calorimetry (ITC) at 25°C.
[a]K_D-values for adenosine, NAD and GDP are estimated to be higher than 100 μM, as their ITC binding curves show weak binding and the isotherm cannot be fitted. Stoichiometries and Δ*H* values could not be determined (ND), due to binding below this ITC detection limit.

contacts with the *macro* domain fold, as its removal reduces affinity 45-fold.

Removal of the β-phosphate of ADP (to give AMP) reduces binding further (Figure 3B). The affinity of AMP is 38.0 μM (Δ*H* = −9.7±1.1 kcal/mol), an additional seven-fold decrease in affinity compared to ADP. We could not observe an interaction between Af1521 and adenosine, suggesting that the two phosphate groups are important (Table I). Likewise, ATP has a reduced affinity compapred to ADP, suggesting that the ligand binding pocket is not designed to accommodate a third phosphate group (Table I).

The Af1521 *macro* domain therefore displays a preference for a diphosphate and a distal ribose ring. In addition, the *macro* domain of Af1521 is specific for the adenine base. The purine-analog guanine, in fact, cannot substitute for the adenine. We are unable to detect an interaction between Af1521 and GDP (Table I). Similarly, only limited binding affinity is observed between Af1521 and NAD^+ (Figure 3C).

In summary, the Af1521 *macro* domain shows selectivity toward the nucleotide ADP-ribose. The observed high affinity and high enthalpy for ADP-ribose suggest that the Af1521

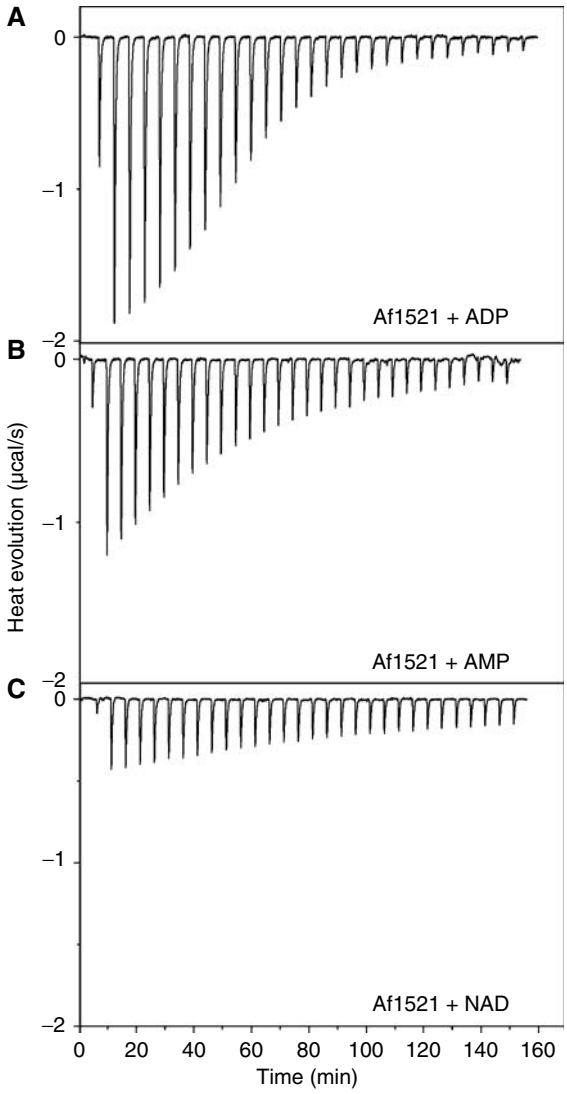

Figure 3 The *macro* domain ligand binding pocket is selective for ADP-ribose. Isothermal titration calorimetry profiles for the binding of (**A**) ADP, (**B**) AMP and (**C**) NAD to the Af1521 *macro* domain protein. Reaction conditions were identical to those of Figure 2. The graphs clearly show decreased affinities of the *macro* domain for these nucleotide ligands compared to ADP-ribose (Figure 2).

protein has a ligand binding pocket that specifically recognizes this ligand.

Structure reveals a highly specific ADP-ribose binding pocket

The isothermal titration calorimetry (ITC) binding data suggest that the Af1521 *macro* domain evolved as a module that binds ADP-ribose. In an effort to understand substrate specificity at the atomic level, we solved the crystal structures of Af1521 bound to two of its ligands. Af1521 has a mixed α/β fold (a single, seven-stranded mixed β-sheet, sandwiched in by four helices) similar to other proteins that bind nucleotides, such as RecA (Story and Steitz, 1992), the F1 ATPase (Abrahams *et al*, 1994; Bauer *et al*, 2001) and CobA. We present the structure of Af1521 bound to the high-affinity ADP-ribose ligand (1.5 Å) and Af1521 bound to ADP (2.5 Å) (Figure 4).

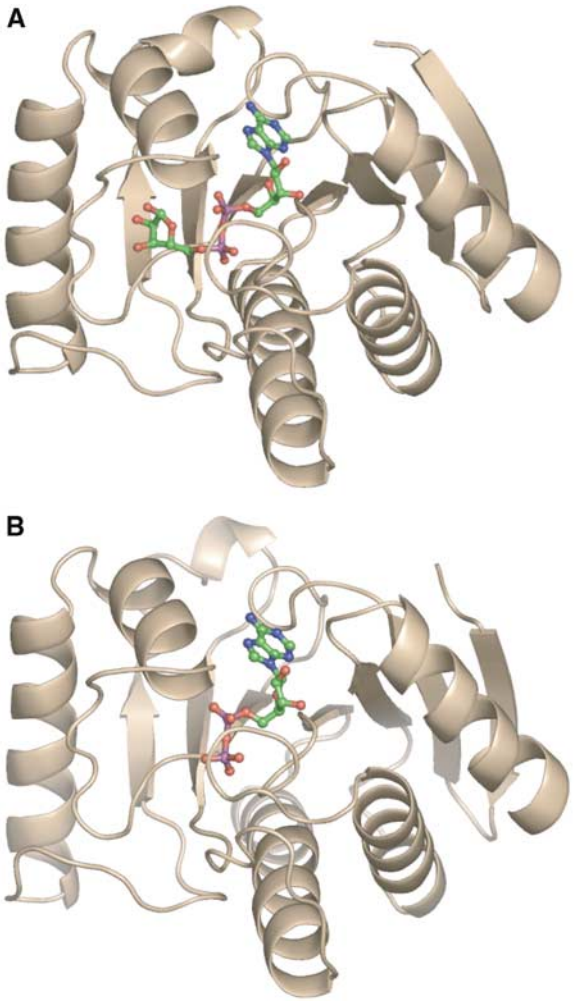

Figure 4 Structure of the complex formed between Af1521 and ADP-ribose. (**A**) The ADP-ribose molecule binds the Af1521 *macro* domain in an L-shaped cleft. The ADP-ribose ligand is shown as a ball-and-stick model. (**B**) Structure of the complex between Af1521 and ADP. The structure is highly similar to that of the complex between Af1521 and ADP-ribose, but a number of interactions that contribute to ADP-ribose specificity and affinity cannot occur. The ADP ligand is shown as a ball-and-stick model.

The ADP-ribose molecule binds Af1521 in an L-shaped cleft on the protein surface at the C-terminus of the α/β unit (Figure 4A). The ADP-ribose complexed Af1521 is highly similar in structure to the nucleotide-free structure (RMSD between Cα positions is small, see Materials and methods). The adenine moiety fits into a deep hydrophobic pocket, formed by residues in the loop between the second and third β-strands, helix 1 and the loop between the final strand of the sheet and the C-terminal helix. The aromatic Tyr 176 stacks onto one side of the adenine ring and the side chains of Val 43 and Ile 21 pack onto the other side (Figure 5). The N6 nitrogen of the adenine is H-bonded to the side chain of Asp 20 and the N1 nitrogen is H-bonded to the backbone HN of Ile 21. Both residues are at the N-terminus of the 3_{10} helix in the loop between the second and third β-strands. The selectivity for adenine over guanine in the ADP and GDP binding assays is accounted for by the presence of these H-bonds and by steric constraints for a carbonyl at the C2 position. There is little contact between Af1521 and the proximal ribose on the ADP portion of the ADP-ribose ligand.

Af1521 shows some similarity to P-loop phosphohydrolases (Allen *et al*, 2003). Many of these proteins interact with phosphate groups through a so-called P-loop motif. The loop between strand 2 and the 3_{10} helix in Af1521 shows some sequence similarity to the P-loop motif, yet in the Af1521 structure this region interacts with the adenine ring, as mentioned above. The phosphates, in fact, form H-bonds to the backbone NH groups of residues in the loop between strand 6 and helix 4. The first phosphate group also H-bonds with the HN of Val 43 at the N-terminus of helix 1. In addition, the phosphate is stabilized by the helix dipole. Overall, the Af1521 *macro* domain is well suited for the binding of ADP-ribose.

Recognition of the distal ribose contributes to specificity

Our binding assays show a 45-fold selectivity of the Af1521 *macro* domain toward ADP-ribose compared to ADP. Consistently, the second, distal ribose ring fits into a specific pocket formed by Tyr 145 and Ile 144 in the loop between strand 6 and helix 4, as well as Ala 44 in helix 1 (Figure 5B). Residues that precede helix 1 form H-bonds to the pyranose ring. The NH_2 group on the Asn 34 side chain, H-bonds to the O3′ oxygen, while the backbone HN of Gly 41 H-bonds to the O1′ oxygen.

While ADP binds Af1521 like ADP-ribose (Figure 4B), the H-bonds that are made to the distal ribose in the ADP-ribose complex are not present in the ADP-bound structure. Consistently, mutation of the Asn 34 to Ala reduces affinity of Af1521 for ADP-ribose three-fold to 390 ± 50 nM, while ADP binding is not affected (Table II). Moreover, mutation of Asp 20, whose side chain makes a hydrogen bond to the NH2 group on the adenine ring, greatly reduces affinity to both ADP-ribose (Table II) and ADP (no binding detected). This suggests that the interaction is critical for nucleotide recognition. The *macro* domain thus makes a number of highly specific noncovalent interactions with the distal ribose and the two phosphate groups (Figure 5C), consistent with the high affinity and specificity for ADP-ribose (Table II).

Macro domains share a conserved ligand binding pocket

There is a significant degree of sequence variation among distinct *macro* domains. Several areas of high sequence conservation are observed and these regions cluster around the Af1521-ADP-ribose binding site (Figure 6A). The hydrophobic residues that line the adenine and ribose binding pockets are generally conserved or replaced with other hydrophobic amino acids. The two amino acids whose side chains directly H-bond the ligand, Asp 20 and Asn 34, are highly conserved. Where these two residues are not conserved, they are replaced by equivalent interactions. Other protein–ligand interactions involve the protein backbone (Figure 5). For these contacts to be maintained, the fold only needs a similar structure in these regions. Generally, such a requirement does not impose a high degree of sequence conservation. Our structural studies suggest that ADP-ribose binding may be a general feature of *macro* domains.

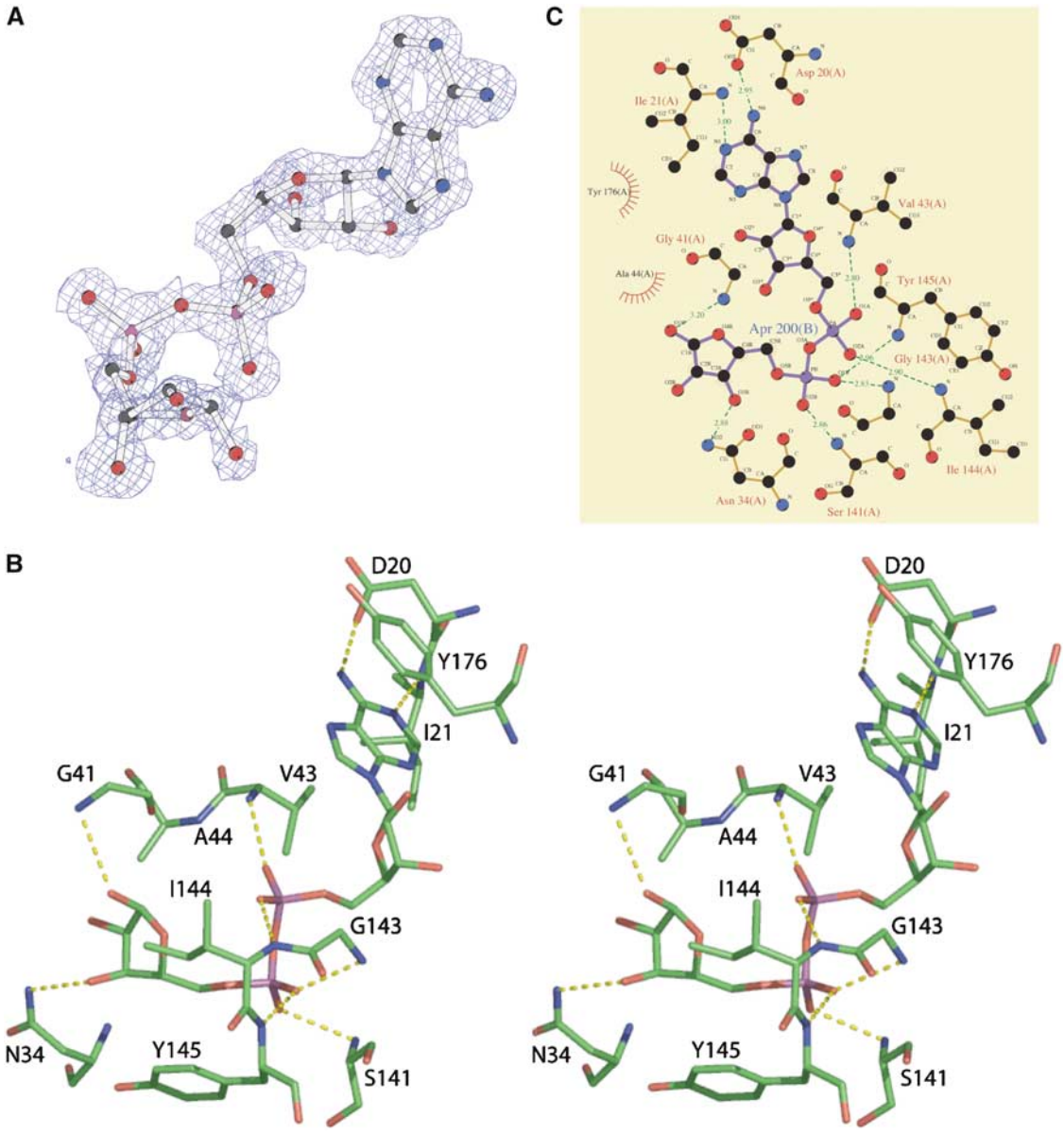

Figure 5 Specificity of the *macro* domain fold for ADP-ribose. (**A**) Electron density for the ADP-ribose ligand in the pocket of the Af1521 protein. The ADP-ribose ligand is shown as a ball-and-stick model. (**B**) Stereo-diagram of the ADP-ribose binding pocket. A number of critical interactions between the ligand and the Af1521 *macro* domain are shown. Several of the interactions involve hydrogen bonds between side chains (Asn 34, Asp 20) and backbone amide bonds. Specific aromatic stacking interactions occur between Tyr 176 and the adenine base. The phosphates are stabilized by a number of interactions, including the backbone amide of Val 43, Ser 141 and the favorable dipole of helix 1. (**C**) Schematic representation for the binding of ADP-ribose to the *macro* domain. The LigPlot (Wallace *et al*, 1995) diagram summarizes key noncovalent interactions between the ADP-ribose ligand and the Af1521 *macro* domain. Legend: thick blue lines, ADP-ribose ligand; thin red lines, *macro* domain residues; circles or semicircles with radiating lines; atoms or residues involved in hydrophobic contacts between protein and ligand.

Conserved macro domains bind ADP-ribose

Our analysis suggests that the *macro* domain of Af1521 has evolved as a module that can bind ADP-ribose. Remarkably, the residues forming the ADP-ribose binding pocket in the Af1521–ADP-ribose complex are conserved across different *macro* domain folds (Figure 6A and B).

We tested whether other *macro* domain proteins might also recognize ADP-ribose. We expressed GST or histidine-tagged fusion proteins of Af1521, yeast YBR022W and three unrelated human *macro* domain proteins. We included, the *macro* domain from Alc1, a putative Snf2-helicase (Guan and Sham, 2003), the *macro* domain of macroH2A (Pehrson and Fried, 1992), a histone variant thought to be involved in transcriptional repression and the *macro* domain from Bal/PARP9 (Ame *et al*, 2004), a PARP involved in leukemia (Aguiar *et al*, 2000). We immobilized these proteins, as well as two controls (pure GST and a GST-fusion of the double bromodomain module of $TAF_{II}250$ (hTaf1), an unrelated module that binds acetylated histones (Jacobson *et al*, 2000; Ladurner *et al*, 2003)). Next, we incubated equimolar amounts of immobilized fusion protein and ADP-ribose. The beads were pelleted and the amount of ADP-ribose retained by the fusion proteins was calculated based on the ADP-ribose left in the supernatant. The pulldown assays show that

Table II Site-directed mutagenesis of the ligand binding pocket in the Af1521 *macro* domain

Protein	K_D (μM)[a]	$\Delta\Delta G$ (kcal/mol)
Wild type	0.13±0.02	—
D20A	11.7±2.1	2.7±0.4
N34A[b]	0.39±0.05	0.7±0.1
Y176L	0.23±0.05	0.3±0.1

Equilibrium values for binding of ADP-ribose to Af1521 protein constructs were determined by isothermal titration calorimetry at 25°C.
[a]$\Delta\Delta G$ (kcal/mol) is the change in the stability of the protein–ligand complex relative to the wild-type protein; $\Delta\Delta G = -RT\ln(K_{\text{wild type}}/K_{\text{Mutant}})$, where R is the universal gas constant, T is the temperature in Kelvin and K is the reciprocal of the equilibrium dissociation constant K_D.
[b]In contrast to ADP-ribose, the N34A mutant recognizes ADP with the same affinity as the wild-type protein (data not shown).

immobilized *macro* domain proteins can retain ADP-ribose (Figure 6C). In contrast, the control proteins do not. Although these assays are not quantitative and not as robust as ITC analysis, ADP-ribose binding could thus be a feature that is shared by several other *macro* domains.

Af1521 and Bal macro domains bind PAR

While there are biological pathways that produce monomeric ADP-ribose, we extended our studies to include its polymeric form, PAR. We tested whether Af1521 recognizes PAR. Since pure, unbranched polymer sufficient for ITC analysis is not available, we have used a classical filter binding assay, which uses ^{32}P-radiolabeled poly-ADP-ribosylated PARP1, generated *in vitro*. The PAR polymer has been reported to bind several histones through a positively charged and hydrophobic sequence (Panzeter and Althaus, 1990; Pleschke *et al*, 2000). We have included histone H2A as a positive control for PAR binding. Lysozyme, which has a highly charged surface, was used as a negative control. Both H2A and the *macro* domain of Af1521 bind PAR polymer (Figure 7). The observed signal is not due to binding of ^{32}P-NAD, but represents PAR polymer, as evidenced by an extensive PAR ladder in sequencing gels (data not shown). Free PAR, that is PAR in the absence of PARP1 protein, also binds the *macro* domain (data not shown). In addition, the double *macro* domain module of Bal/PARP9, recognizes PAR (Figure 7). PAR binding to Af1521 and to Bal/PARP9 *macro* domains resists repeated, high-stringency salt washes. In addition, the PAR polymer binds the two tested proteins also as a protein-free polymer (data not shown). Together, this suggests that *macro* domains recognize and bind PAR.

Discussion

Macro domains are high-affinity ADP-ribose binding modules

Our data provide evidence that the widespread *macro* domain evolved as a module that binds ADP-ribose with high specificity. Af1521 binds ADP-ribose with nanomolar affinity. The existence of a number of critical noncovalent interactions is observed in the crystal structure of the ADP-ribose complex. Site-directed mutants also reveal a ligand binding pocket that makes a number of important contacts with structural element of the ADP-ribose moiety, except for the proximal ribose, which is accommodated loosely. Furthermore, other *macro* domains, including those from three human proteins, interact with ADP-ribose. Together, our data suggest that the recognition of ADP-ribose is a key function of the *macro* domain.

We also show that Af1521 and YBR022W, albeit slowly, can hydrolyze the phospho-monoester in ADP-ribose-1″-phosphate and that the reaction products are ADP-ribose and inorganic phosphate. The ability of the Af1521 and YBR022W *macro* domains to catalyze a phosphohydrolase reaction does not prove that these *macro* domains (or *macro* domains, in general) are genuine enzymes *in vivo*. Enzyme activity here may be rather promiscuous.

Further, *macro* domains exhibit a well-conserved ADP-ribose ligand binding pocket. The two tested *macro* domains also bind PAR. Since *macro* domains are associated with a diverse range of biological processes, this suggests that ADP-ribose and related ligands may be important in mediating the different biological responses.

Macro domains may act in distinct ADP-ribose pathways

The ability of three distinct human *macro* domain proteins to recognize ADP-ribose is interesting. First, ADP-ribose binding may affect the function of the Alc1 protein. As Alc1 shows homology to the Snf2 helicase of the Swi/Snf chromatin remodeling factor, ADP-ribose may be involved in chromatin remodeling. Unrelated inositol polyphosphate nucleotides are involved in the regulation of the Swi/Snf remodeller (Shen *et al*, 2003; Steger *et al*, 2003). Second, the ability of immobilized macroH2A *macro* domain to precipiate ADP-ribose suggests that this histone could bind this or related nucleotides. Third, the recognition of both ADP-ribose and PAR by Bal/PARP9, suggests that this PARP enzyme may benefit from its ability to recognize the product of its own reaction. PAR consists of ADP-ribose units connected between the 2′-OH (on the proximal ribose) and the 1″-OH (on the distal ribose). Both these groups point away from the structure and are accessible to solvent in the ADP-ribose–Af1521 complex. Specific structural and steric constrains may have to be met for *macro* modules to bind PAR. In fact, as *macro* domains vary considerably in structure outside of the core ADP-ribose ligand binding pocket (Figure 6A and B), it is possible that PAR binding may not be a general property of *macro* domains.

The filter binding assay cannot determine whether Af1521 and Bal/PARP9 *macro* domains recognize PAR along the polymer or cap the last ADP-ribose on the polymer. However, the presence of two *macro* domains in Bal/PARP9 would be more consistent with an interaction along the polymer. This feature could promote PARP activity. Consistently, the two other human PARP enzymes that contain *macro* domains (PARP14 and PARP15; Ame *et al*, 2004), repeat this module two and three times, respectively.

The functional coupling of an enzymatic domain with a domain that recognizes the enzyme's product is a common feature of proteins. Several histone acetyltransferases, for example, contain bromodomains, motifs that can recognize acetylated lysines (Dhalluin *et al*, 1999; Jacobson *et al*, 2000; Owen *et al*, 2000). This may improve the processivity of enzymes such as PARP. The existence and functional

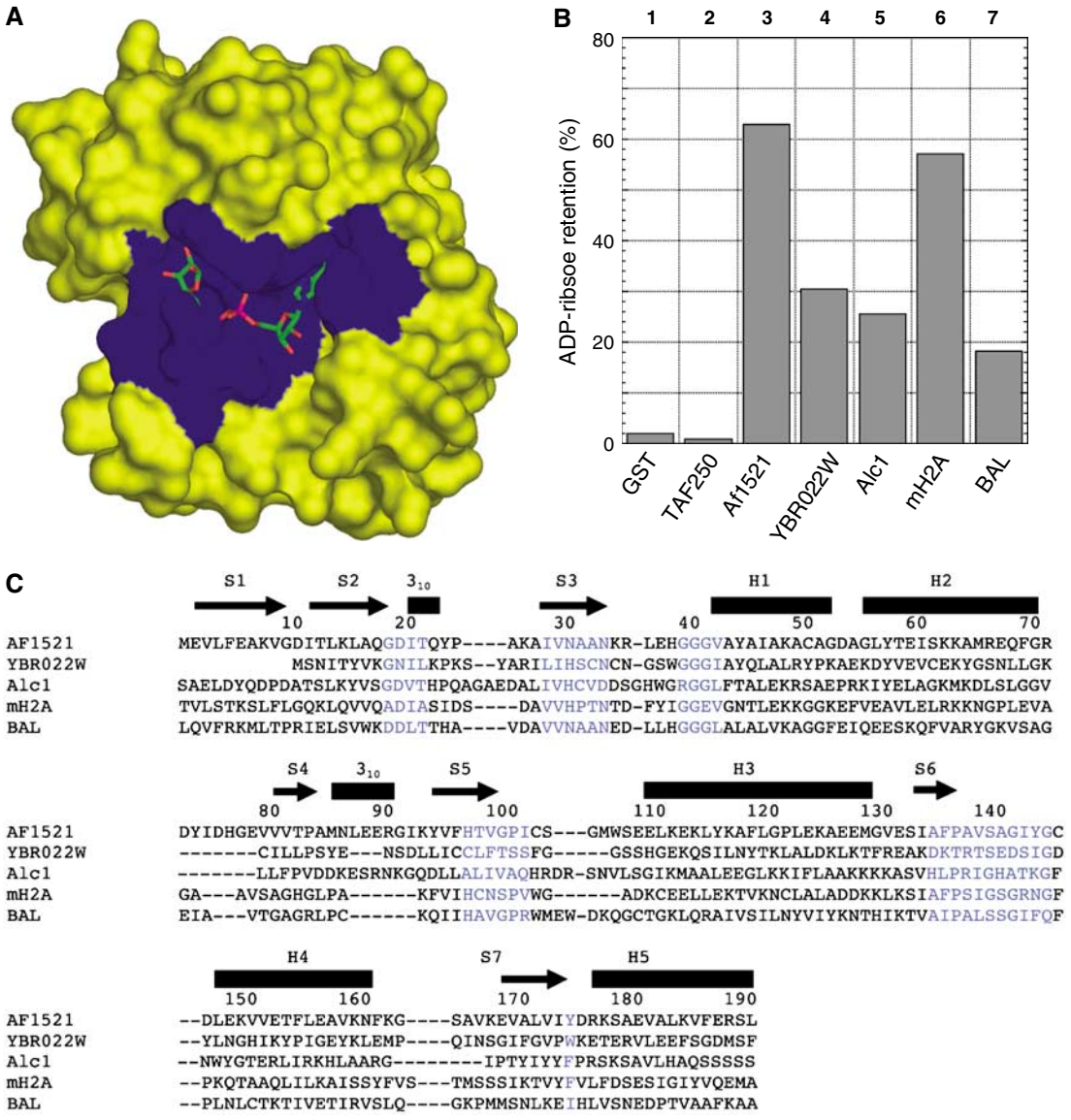

Figure 6 ADP-ribose binding is a conserved feature among *macro* domains. (**A**) Sequence and structure conservation in the *macro* domain family of proteins. Regions with the highest sequence conservation among *macro* domain proteins are shown in blue. These include residues (19–22), (29–34), (40–43), (98–103), (136–146) and 176. (**B**) Structure-guided alignment between select *macro* domain proteins. For the purpose of this alignment, only the *macro* domains used in this study were aligned. The alignment was generated using the output of a Blast search, and refined manually on the Af1521–ADP-ribose complex structure. Residues shown in blue correspond to the region colored in blue of panel (A). (**C**) Pulldown assays for the binding of ADP-ribose to yeast and human *macro* domains. Distinct *macro* domain proteins (*A. fulgidus* Af1521, *S. cerevisiae* YBR022W, human Alc1, human macroH2A and human BAL/PARP9) were fused to either GST protein or to a histidine-tag. In all, 30 nmol of fusion proteins was immobilized to a solid support, including two control proteins that should not interact with ADP-ribose (GST and a GST-fusion of the $TAF_{II}250$ (hTAF1) double bromodomain module (Jacobson *et al*, 2000)), and incubated with 30 nmol of ADP-ribose in solution. Following the incubation, the samples were centrifuged and the amount of ADP-ribose that remained in the supernatant was estimated by absorbance measurements. The graphs show the percentage retention on the beads (calculated by subtracting the percentage of ADP-ribose that remained in the supernatant from 100%). The pulldown assay shows that all tested *macro* domain proteins retain some ADP-ribose.

consequences of such a mechanism remain to be tested for PARPs.

Our structure/function study reveals a structural motif capable of recognizing monomeric and also polymeric ADP-ribose. *Macro* domains may thus provide a molecular link between distinct molecular forms of ADP-ribose and key biological pathways. The coming years will see the emergence of detailed molecular and mechanistic insight into the biology of NAD and its important cellular metabolites.

Materials and methods

Protein expression and purification

Expression, purification and thrombin-cleavage of the $(His)_6$-Af1521 has been described (Allen *et al*, 2003). All other constructs were generated by PCR with Phusion polymerase (Finnzymes, Finland) and oligos (Sigma Genosys, Germany), using *S. cerevisiae* genomic DNA (for YBR022W) or EST templates (RZPD, Germany). GST, GST-fusions of $hTAF_{II}250$ (hTaf1) double bromodomain and GST fusions of Alc1, macroH2A and Bal/PARP9 *macro* domains were expressed in *Rosetta* cells (Novagen, USA) at 22°C for 12 h with 200 μM IPTG induction. Cell harvest was snap frozen on liquid N_2, resuspended

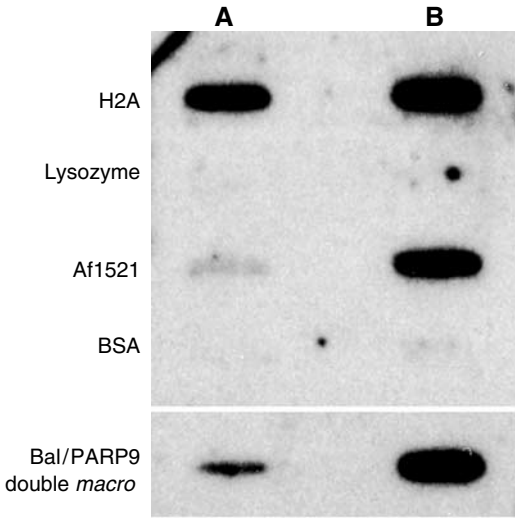

Figure 7 The Af1521 and human Bal/PARP9 *macro* domains recognize poly-ADP-ribosylated PARP1. ^{32}P-labelled PAR-labelled PARP1 was incubated on nitrocellulose filter papers containing slot-blotted proteins. The membranes contained 20 pmol (lane A) and 200 pmol (lane B) of H2A, Af1521 *macro* domain and human Bal/PARP9 double *macro* domain module, as well as 200 pmol (lane A) and 400 pmol (lane B) of the control proteins lysozyme and BSA. After extensive washes, the filter membranes were dried and autoradiographed. Incubation of ^{32}P-NAD with the slot-blotted proteins produced no signal (data not shown). The loading of slot-blotted proteins was verified using Sypro Ruby protein blot stain.

Table III Crystallographic data and refinement statistics

	ADP-ribose/ Af1521	ADP/Af1521
Data collection		
Space group	$P6_1$	$P6_1$
Wavelength (Å)	0.934	0.934
Resolution range (Å)	23.4–1.5	28.7–2.5
Unique reflections	41551	9073
Completeness (%)[a]	97.0 (98.3)	96.1 (97.1)
R_{merge}[b]	0.054 (0.262)	0.065 (0.238)
Multiplicity[c]	4.8 (4.7)	2.4 (2.3)
$I/\sigma I$[1]	18.3 (5.3)	12.2 (4.7)
Cell dimensions *a,b,c* (Å)	88.12, 88.12, 60.28	87.84, 87.84, 61.07
Refinement		
Resolution (Å)	20.0–1.5	25.0–2.5
No. of reflections (working/free)	39391/2041	8528/483
No. of residues	A: 1–192	A: 1–192
No. of water, ligands	155, 1 ADP-ribose	40, 1 ADP
R_{work}/R_{free}[a]	0.201, 0.232	0.202, 0.237
B average[b]	24.4 Å[a]	34.8 Å[b]
Geometry bonds/angles[d]	0.012 Å, 1.590°	0.005 Å, 1.127°
Ramachandran[c]	95.8%/0.6% (1 residue/ chain)	91.1%/0.6% (1 residue/ chain)
PDB ID code[e]	2BFQ	2BFR

[a]5% of reflections were randomly selected for determination of the free *R*-factor, prior to any refinement.
[b]Temperature factors averaged for all atoms.
[c]Percentage of residues in the 'most favored region' of the Ramachandran plot and percentage of outliers (PROCHECK).
[d]RMS deviations from ideal geometry for bond lengths and restraint angles.
[e]Protein Data Bank identifiers for coordinates.

in ice-cold lysis buffer (50 mM Tris–Hcl, pH 7.9, 0.1 mM EDTA, 0.5 M NaCl, 10% glycerol, 1 mM DTT and protease inhibitors), lysed in an Emulsiflex-C5 (Avestin, Canada), sonicated for 3 × 20 s at medium setting (Brandon, USA) and centrifuged for 20 min at 16 000 r.p.m. in a SS34 rotor. The supernatant was incubated with glutathione sepharose (Amersham Biosciences, Sweden). Beads were washed 5 × with 45 ml of lysis buffer containing 1 M NaCl and re-equilibrated 2 × with a buffer containing 50 mM NaCl. For ADP-ribose pulldown assays, protein concentration was determined by Coomassie staining relative to BSA standards, or by absorbance measurements. The concentration of purified, soluble Af1521 was determined using the molar extinction coefficient $\varepsilon^{280} = 17\,795$ OD/M/cm. For the PAR interaction assays, the Bal/PARP9 double *macro* module was cleaved from GST using thrombin. *Xenopus laevis* H2A was purified as published (Luger *et al*, 1997, 1999).

Catalytic and binding assays

Detection of catalysis by Af1521 was carried out using TLC and malachite green assays. Briefly, 2 mM ADP-ribose 1″–2″-cyclic phosphate (Appr > P) was incubated with 6 μg of cyclic phosphodiesterase (in 9 μl volume) to produce Appr-1″-phosphate. To this, we added 1 μl of calf intestine alkaline phosphatase (MBI Fermentas, Lithuania) or of *macro* domain (6 μg) for 12 h at 30°C. Following incubation, 2 μl were mixed with 1 μl of 100 mM tetrabutylammonium, and the sample applied to an Alugram Nano-SIL CN/UV_{254} TLC plate (Macherey Nagel, Germany) and run at room temperature using an aqueous solution containing 1.5 M LiCl and 20% v/v ethanol. Digital fluorescence pictures were taken with a UV lamp at 254 nm wavelength.

Inorganic phosphate was detected using a malachite green assay. Briefly, 800 μl of samples contained 172 μl of 28 mM ammonium heptamolybdate in 2.1 M H_2SO_4, 128 μl of 0.76 mM malachite green solution in 0.35% polyvinyl alcohol (~16 000 MW) and varying amounts of either KP_i standards or Af1521-catalyzed reaction and controls. Absorbance was measured at 610 nm wavelength following a 20-min incubation at 22°C.

Isothermal titration binding assays were carried out at 25°C using a VP-ITC instrument (MicroCal, USA). Binding reactions were carried out in 50 mM KP_i buffer (pH 6.5), using 10–50 μM Af1521 *macro* domain and different nucleotides (Sigma, USA). Ligands in the injection syringe were at a concentration that exceeded the concentration of Af1521 8 to 15 times (150–750 μM). Data analysis was conducted using Origin software (OriginLab, USA).

ADP-ribose pulldown assays were performed using 30 nmol of immobilized fusion protein (~50 μl bead volume) in a 1 ml total sample volume. The buffer was 1 × PBS, 1 mM DTT. The concentration of ADP-ribose was 30 μM. Following the incubation of the ADP-ribose and immobilized protein at 22°C (RT) for 30 min, the sample was centrifuged and the amount of ADP-ribose remaining in the supernatant was determined using absorbance measurements (OD) at 260 nm wavelength. The percentage retention was calculated by comparing the OD of the supernatants with the OD of a 30 μM ADP-ribose sample. For a *macro* domain–ADP-ribose complex with 1:1 stoichiometry and infinitely high affinity, a theoretical retention of 100% would be expected.

PAR binding assays

PAR binding assays were performed essentially as described (Malanga *et al*, 1998), using PARP1-bound polymer. In all, 20 and 200 pmol of H2A, Af1521 and human Bal/PARP9 were blotted on nitrocellulose membranes using a Minifold II slot blot apparatus (Schleicher & Schuell) and 200 and 400 pmol were blotted for both lysozyme and BSA controls. The membranes were blocked in TBS-T buffer (10 mM Tris, pH 7.4, 150 mM NaCl, 0.05% Tween 20) containing 5% dry milk powder. Enzymatic reactions were set up as described (Panzeter *et al*, 1992). The enzymatic reactions were set up using 0.4 U of bovine PARP-1 (Biomol), 6 μg/ml activated calf-thymus DNA (Sigma), 150 μM NAD^+ spiked with [^{32}P]-NAD^+ (Amersham Biosciences, UK). The final specific activity of the NAD^+ was 0.5 μCi per nmol NAD^+, in 25 mM Tris (pH 8.0), 10 mM $MgCl_2$, 0.1 M NaCl, 0.5 mM DTT. The reaction mix was incubated for 1 h at 25°C, then diluted to 10 ml with TBS-T and incubated with the slot blot membranes for 1 h at 25°C under constant agitation. Afterwards, the membranes were washed twice for 10 min with 10 ml TBS-T and five times for 5 min with 10 ml TBS-T, and then three times for 5 min with TBS-T containing 1 M NaCl. The membranes were air-dried and autoradiographed. Subsequently,

the membranes were stained with Sypro Ruby (BioRad) according to the manufacturer's instructions. In separate experiments, we also detached the PAR polymer from the activated bovine PARP1, using 1 U of DNAseI (Fermentas) to the reaction after 60 min, and incubated for 10 min at 37°C. Next, 50 U of proteinase K (Roche) was added, followed by 30 min at 37°C. After phenol–chloroform extraction, the water-soluble polymer was diluted to 10 ml with TBS-T and incubated with the slot-blotted proteins. Binding to macro domains under these conditions provided highly similar results (data not shown).

Crystallization, data collection and processing

Crystals of the AF1521/ADP-ribose complex were obtained in sitting drops at 25°C by mixing equal volumes of a precipitant solution consisting of 30% (w/v) PEG 4000 (Hamilton Research), 0.2 M ammonium acetate and 0.1 M tri-sodium citrate (pH 5.6) with a solution containing protein at 18 mg/ml, 1.5 mM ADP-ribose, 5 mM DTT and Tris buffer at pH 7.0. Crystal mother liquor containing 20% (v/v) glycerol was used as cryoprotectant.

Crystals of the AF1521/ADP complex were obtained in sitting drops at 25°C by mixing equal volumes of a precipitant solution consisting of 20% (w/v) PEG 8000 (Hamilton Research), 0.2 M magnesium acetate, and 0.1 M sodium cacodylate (pH 4.5) with a solution containing protein at 18 mg/ml, 1.5 mM ADP, 5 mM DTT and Tris buffer at pH 7.0. Crystal mother liquor containing 20% (v/v) glycerol was used as a cryoprotectant solution.

All crystals were frozen in liquid N_2 after soaking in cryoprotectant. Data collection was carried out at 100 K using beamline 14.1 at the European Synchrotron Radiation Facility as an X-ray source. X-ray diffraction data were indexed and integrated using the MOSFLM package (Leslie, 1991) and processed using CCP4 (Collaborative Computational Project, 1994).

The structures of the ADP and ADP-ribose complexes were solved by molecular replacement using the structure of MES-bound Af1521 and the program CNS (Brunger *et al*, 1998). The structures were built using MAIN (Turk, 1992) and refined using CNS with Engh and Huber stereochemical parameters. Details of the final models are summarized in Table III. The RMSD between Cα positions in the ADP or ADP-ribose-bound Af1521 structure and that of the Mes-bound Af1521 (Allen *et al*, 2003) are small. There are two molecules in the Mes-bound structure, Af1521 molecule (A) and molecule (B). The RMSD between Mes-Af1521 (A) and Mes-Af1521 (B) is 0.37 Å, between Mes-Af1521 (A) and the ADP-ribose-bound Af1521 it is 0.47 Å, and between Mes-Af1521 (B) and ADP-ribose-bound Af1521 it is 0.27 Å.

Coordinates

The atomic coordinate and structure factors for the ADP-ribose-Af1521 and ADP-Af1521 complexes have been deposited in the Protein Data Bank (accession codes 2BFQ and 2BFR, respectively).

Acknowledgements

This work was supported by the EMBL and by the MRC. We thank W Filipowicz for the gift of Appr>P compound and cyclic phosphodiesterase enzyme, C Schultz for advice on ADP-ribose chemistry, K Luger and T Richmond for the H2A expression construct, M Knop for *S. cerevisiae* DNA, E Izaurralde for the slot-blot apparatus and M-B Hansen for photography. GIK and HRB were trainee undergraduates and we are grateful to R Sandaltzopoulos and F Hollfelder for coordinating their placements.

References

Abrahams JP, Leslie AGW, Lutter R, Walker JE (1994) Structure at 2.8 Angstrom resolution of the F1-ATPase from bovine heart mitochondria. *Nature* **370:** 621–628

Adamietz P, Rudolph A (1984) ADP-ribosylation of nuclear proteins *in vivo*. Identification of histone H2B as a major acceptor for mono- and poly(ADP-ribose) in dimethyl sulfate-treated hepatoma AH 7974 cells. *J Biol Chem* **259:** 6841–6846

Aguiar RC, Yakushijin Y, Kharbanda S, Salgia R, Fletcher JA, Shipp MA (2000) BAL is a novel risk-related gene in diffuse large B-cell lymphomas that enhances cellular migration. *Blood* **96:** 4328–4334

Allen MD, Buckle AM, Cordell SC, Lowe J, Bycroft M (2003) The crystal structure of AF1521 a protein from *Archaeoglobus fulgidus* with homology to the non-histone domain of macroH2A. *J Mol Biol* **330:** 503–511

Ame JC, Spenlehauer C, de Murcia G (2004) The PARP superfamily. *Bioessays* **26:** 882–893

Aravind L (2001) The WWE domain: a common interaction module in protein ubiquitination and ADP ribosylation. *Trends Biochem Sci* **26:** 273–275

Bauer CB, Fonseca MV, Holden HM, Thoden JB, Thompson TB, Escalante-Semerena JC, Rayment I (2001) Three-dimensional structure of ATP:corrinoid adenosyltransferase from *Salmonella typhimurium* in its free state, complexed with MgATP, or complexed with hydroxycobalamin and MgATP. *Biochemistry* **40:** 361–374

Beneke S, Diefenbach J, Burkle A (2004) Poly(ADP-ribosyl)ation inhibitors: promising drug candidates for a wide variety of pathophysiologic conditions. *Int J Cancer* **111:** 813–818

Benjamin RC, Gill DM (1980) Poly(ADP-ribose) synthesis *in vitro* programmed by damaged DNA. A comparison of DNA molecules containing different types of strand breaks. *J Biol Chem* **255:** 10502–10508

Brunger AT, Adams PD, Clore GM, DeLano WL, Gros P, Grosse-Kunstleve RW, Jiang JS, Kuszewski J, Nilges M, Pannu NS, Read RJ, Rice LM, Simonson T, Warren GL (1998) Crystallography & NMR system: a new software suite for macromolecular structure determination. *Acta Crystallogr D Biol Crystallogr* **54** (Part 5)**:** 905–921

Cervellera MN, Sala A (2000) Poly(ADP-ribose) polymerase is a B-MYB coactivator. *J Biol Chem* **275:** 10692–10696

Chadwick BP, Willard HF (2001) Histone H2A variants and the inactive X chromosome: identification of a second macroH2A variant. *Hum Mol Genet* **10:** 1101–1113

Chambon P, Weill JD, Mandel P (1963) Nicotinamide mononucleotide activation of a new DNA-dependent polyadenylic acid synthesizing nuclear enzyme. *Biochem Biophys Res Commun* **11:** 39–43

Chang P, Jacobson MK, Mitchison TJ (2004) Poly(ADP-ribose) is required for spindle assembly and structure. *Nature* **432:** 645–649

Chiarugi A (2002) Poly(ADP-ribose) polymerase: killer or conspirator? The 'suicide hypothesis' revisited. *Trends Pharmacol Sci* **23:** 122–129

Cohen-Armon M, Visochek L, Katzoff A, Levitan D, Susswein AJ, Klein R, Valbrun M, Schwartz JH (2004) Long-term memory requires polyADP-ribosylation. *Science* **304:** 1820–1822

Collaborative Computational Project, N (1994) The CCP4 suite: programs for protein crystallography. *Acta Crystallogr D Biol Crystallogr* **50:** 760–763

Cook BD, Dynek JN, Chang W, Shostak G, Smith S (2002) Role for the related poly(ADP-Ribose) polymerases tankyrase 1 and 2 at human telomeres. *Mol Cell Biol* **22:** 332–342

Corda D, Di Girolamo M (2003) Functional aspects of protein mono-ADP-ribosylation. *EMBO J* **22:** 1953–1958

Culver GM, McCraith SM, Zillmann M, Kierzek R, Michaud N, LaReau RD, Turner DH, Phizicky EM (1993) An NAD derivative produced during transfer RNA splicing: ADP-ribose 1″–2″ cyclic phosphate. *Science* **261:** 206–208

D'Amours D, Desnoyers S, D'Silva I, Poirier GG (1999) Poly(ADP-ribosyl)ation reactions in the regulation of nuclear functions. *Biochem J* **342:** 249–268

Davidovic L, Vodenicharov M, Affar EB, Poirier GG (2001) Importance of poly(ADP-ribose) glycohydrolase in the control of poly(ADP-ribose) metabolism. *Exp Cell Res* **268:** 7–13

Dhalluin C, Carlson JE, Zeng L, He C, Aggarwal AK, Zhou MM (1999) Structure and ligand of a histone acetyltransferase bromodomain. *Nature* **399:** 491–496

Durkacz BW, Omidiji O, Gray DA, Shall S (1980) (ADP-ribose)n participates in DNA excision repair. *Nature* **283:** 593–596

Dynek JN, Smith S (2004) Resolution of sister telomere association is required for progression through mitosis. *Science* **304:** 97–100

Earle E, Saxena A, MacDonald A, Hudson DF, Shaffer LG, Saffery R, Cancilla MR, Cutts SM, Howman E, Choo KH (2000) Poly(ADP-ribose) polymerase at active centromeres and neocentromeres at metaphase. *Hum Mol Genet* **9:** 187–194

Glaser P, Frangeul L, Buchrieser C, Rusniok C, Amend A, Baquero F, Berche P, Bloecker H, Brandt P, Chakraborty T, Charbit A, Chetouani F, Couve E, de Daruvar A, Dehoux P, Domann E, Dominguez-Bernal G, Duchaud E, Durant L, Dussurget O, Entian KD, Fsihi H, Garcia-del Portillo F, Garrido P, Gautier L, Goebel W, Gomez-Lopez N, Hain T, Hauf J, Jackson D, Jones LM, Kaerst U, Kreft J, Kuhn M, Kunst F, Kurapkat G, Madueno E, Maitournam A, Vicente JM, Ng E, Nedjari H, Nordsiek G, Novella S, de Pablos B, Perez-Diaz JC, Purcell R, Remmel B, Rose M, Schlueter T, Simoes N, Tierrez A, Vazquez-Boland JA, Voss H, Wehland J, Cossart P (2001) Comparative genomics of Listeria species. *Science* **294:** 849–852

Guan XY, Sham JST (2003) Homo sapiens ALC1 mRNA. *GenBank*, AF537213

Hanai S, Kanai M, Ohashi S, Okamoto K, Yamada M, Takahashi H, Miwa M (2004) Loss of poly(ADP-ribose) glycohydrolase causes progressive neurodegeneration in *Drosophila melanogaster*. *Proc Natl Acad Sci USA* **101:** 82–86

Hassa PO, Hottiger MO (1999) A role of poly (ADP-ribose) polymerase in NF-kappaB transcriptional activation. *Biol Chem* **380:** 953–959

Ikejima M, Noguchi S, Yamashita R, Ogura T, Sugimura T, Gill DM, Miwa M (1990) The zinc fingers of human poly(ADP-ribose) polymerase are differentially required for the recognition of DNA breaks and nicks and the consequent enzyme activation. Other structures recognize intact DNA. *J Biol Chem* **265:** 21907–21913

Jacobson RH, Ladurner AG, King DS, Tjian R (2000) Structure and function of a human TAFII250 double bromodomain module. *Science* **288:** 1422–1425

Kim H, Jacobson MK, Rolli V, Menissier-de Murcia J, Reinbolt J, Simonin F, Ruf A, Schulz G, de Murcia G (1997) Photoaffinity labelling of human poly(ADP-ribose) polymerase catalytic domain. *Biochem J* **322** (Part 2)**:** 469–475

Kim MY, Mauro S, Gevry N, Lis JT, Kraus WL (2004) NAD+-dependent modulation of chromatin structure and transcription by nucleosome binding properties of PARP-1. *Cell* **119:** 803–814

Kraus WL, Lis JT (2003) PARP goes transcription. *Cell* **113:** 677–683

Krupitza G, Cerutti P (1989) Poly(ADP-ribosylation) of histones in intact human keratinocytes. *Biochemistry* **28:** 4054–4060

Ladurner AG (2003) Inactivating chromosomes: a macro domain that minimizes transcription. *Mol Cell* **12:** 1–3

Ladurner AG, Inouye C, Jain R, Tjian R (2003) Bromodomains mediate an acetyl-histone encoded antisilencing function at heterochromatin boundaries. *Mol Cell* **11:** 365–376

Leslie AGW (1991) *Recent Changes to the MOSFLM Package for Processing of Image-Plate Data*. Daresbury, Warrington: SERC Laboratory

Letunic I, Copley RR, Schmidt S, Ciccarelli FD, Doerks T, Schultz J, Ponting CP, Bork P (2004) SMART 4.0: towards genomic data integration. *Nucleic Acids Res* **32** (Database issue)**:** D142–D144

Lin W, Ame JC, Aboul-Ela N, Jacobson EL, Jacobson MK (1997) Isolation and characterization of the cDNA encoding bovine poly(ADP-ribose) glycohydrolase. *J Biol Chem* **272:** 11895–11901

Luger K, Rechsteiner TJ, Flaus AJ, Waye MM, Richmond TJ (1997) Characterization of nucleosome core particles containing histone proteins made in bacteria. *J Mol Biol* **272:** 301–311

Luger K, Rechsteiner TJ, Richmond TJ (1999) Preparation of nucleosome core particle from recombinant histones. *Methods Enzymol* **304:** 3–19

Malanga M, Pleschke JM, Kleczkowska HE, Althaus FR (1998) Poly(ADP-ribose) binds to specific domains of p53 and alters its DNA binding functions. *J Biol Chem* **273:** 11839–11843

Martzen MR, McCraith SM, Spinelli SL, Torres FM, Fields S, Grayhack EJ, Phizicky EM (1999) A biochemical genomics approach for identifying genes by the activity of their products. *Science* **286:** 1153–1155

McClelland M, Sanderson KE, Spieth J, Clifton SW, Latreille P, Courtney L, Porwollik S, Ali J, Dante M, Du F, Hou S, Layman D, Leonard S, Nguyen C, Scott K, Holmes A, Grewal N, Mulvaney E, Ryan E, Sun H, Florea L, Miller W, Stoneking T, Nhan M, Waterston R, Wilson RK (2001) Complete genome sequence of *Salmonella enterica* serovar Typhimurium LT2. *Nature* **413:** 852–856

Miwa M, Sugimura T (1971) Splitting of the ribose-ribose linkage of poly(adenosine diphosphate-robose) by a calf thymus extract. *J Biol Chem* **246:** 6362–6364

Ogata N, Ueda K, Kagamiyama H, Hayaishi O (1980) ADP-ribosylation of histone H1. Identification of glutamic acid residues 2, 14, and the COOH-terminal lysine residue as modification sites. *J Biol Chem* **255:** 7616–7620

Owen DJ, Ornaghi P, Yang JC, Lowe N, Evans PR, Ballario P, Neuhaus D, Filetici P, Travers AA (2000) The structural basis for the recognition of acetylated histone H4 by the bromodomain of histone acetyltransferase gcn5p. *EMBO J* **19:** 6141–6149

Panzeter PL, Althaus FR (1990) High resolution size analysis of ADP-ribose polymers using modified DNA sequencing gels. *Nucleic Acids Res* **18:** 2194

Panzeter PL, Realini CA, Althaus FR (1992) Noncovalent interactions of poly(adenosine diphosphate ribose) with histones. *Biochemistry* **31:** 1379–1385

Pehrson JR, Fried VA (1992) MacroH2A, a core histone containing a large nonhistone region. *Science* **257:** 1398–1400

Pleschke JM, Kleczkowska HE, Strohm M, Althaus FR (2000) Poly(ADP-ribose) binds to specific domains in DNA damage checkpoint proteins. *J Biol Chem* **275:** 40974–40980

Poirier GG, Niedergang C, Champagne M, Mazen A, Mandel P (1982) Adenosine diphosphate ribosylation of chicken-erythrocyte histones H1, H5 and high-mobility-group proteins by purified calf-thymus poly(adenosinediphosphate-ribose) polymerase. *Eur J Biochem* **127:** 437–442

Rippmann JF, Damm K, Schnapp A (2002) Functional characterization of the poly(ADP-ribose) polymerase activity of tankyrase 1, a potential regulator of telomere length. *J Mol Biol* **323:** 217–224

Rouleau M, Aubin RA, Poirier GG (2004) Poly(ADP-ribosyl)ated chromatin domains: access granted. *J Cell Sci* **117:** 815–825

Ruf A, Rolli V, de Murcia G, Schulz GE (1998) The mechanism of the elongation and branching reaction of poly(ADP-ribose) polymerase as derived from crystal structures and mutagenesis. *J Mol Biol* **278:** 57–65

Saxena A, Wong LH, Kalitsis P, Earle E, Shaffer LG, Choo KH (2002) Poly(ADP-ribose) polymerase 2 localizes to mammalian active centromeres and interacts with PARP-1, Cenpa, Cenpb and Bub3, but not Cenpc. *Hum Mol Genet* **11:** 2319–2329

Shen X, Xiao H, Ranallo R, Wu WH, Wu C (2003) Modulation of ATP-dependent chromatin-remodeling complexes by inositol polyphosphates. *Science* **299:** 112–114

Simonin F, Poch O, Delarue M, de Murcia G (1993) Identification of potential active-site residues in the human poly(ADP-ribose) polymerase. *J Biol Chem* **268:** 8529–8535

Smith S, Giriat I, Schmitt A, de Lange T (1998) Tankyrase, a poly(ADP-ribose) polymerase at human telomeres. *Science* **282:** 1484–1487

Steger DJ, Haswell ES, Miller AL, Wente SR, O'Shea EK (2003) Regulation of chromatin remodeling by inositol polyphosphates. *Science* **299:** 114–116

Story RM, Steitz TA (1992) Structure of the recA protein–ADP complex. *Nature* **355:** 374–376

Tulin A, Spradling A (2003) Chromatin loosening by poly(ADP)-ribose polymerase (PARP) at *Drosophila* puff loci. *Science* **299:** 560–562

Turk D (1992) *Weiterentwicklung eines Programs fuer Molekuelgrafik und Elektrondichte-Manipulation und seine Anwendung auf verschiedene Protein-Strukturaufklaerungen*. Muenchen: Technishe Universitaet

Virag L, Szabo C (2002) The therapeutic potential of poly(ADP-ribose) polymerase inhibitors. *Pharmacol Rev* **54:** 375–429

Wallace AC, Laskowski RA, Thornton JM (1995) LIGPLOT: a program to generate schematic diagrams of protein–ligand interactions. *Protein Eng* **8:** 127–134

Weill JD, Busch S, Chambon P, Mandel P (1963) The effect of estradiol injections upon chicken liver nuclei ribonucleic acid polymerase. *Biochem Biophys Res Commun* **10:** 122–126

Winstall E, Affar EB, Shah R, Bourassa S, Scovassi AI, Poirier GG (1999a) Poly(ADP-ribose) glycohydrolase is present and active in mammalian cells as a 110-kDa protein. *Exp Cell Res* **246:** 395–398

Winstall E, Affar EB, Shah R, Bourassa S, Scovassi IA, Poirier GG (1999b) Preferential perinuclear localization of poly(ADP-ribose) glycohydrolase. *Exp Cell Res* **251:** 372–378

Yu W, Ginjala V, Pant V, Chernukhin I, Whitehead J, Docquier F, Farrar D, Tavoosidana G, Mukhopadhyay R, Kanduri C, Oshimura M, Feinberg AP, Lobanenkov V, Klenova E, Ohlsson R (2004) Poly(ADP-ribosyl)ation regulates CTCF-dependent chromatin insulation. *Nat Genet* **36:** 1105–1110

